Improved Precision Casting of Titanium Alloys Using Calcium Zirconate Moulds

L. Freitag, F. Bulling, U. E. Klotz, St. Schafföner, Chr. G. Aneziris

The main challenges of titanium investment casting are the high melting temperature and the extreme reactivity of the melt. Therefore, a new ceramic material for crucibles and moulds based on calcium zirconate ($CaZrO_3$) is under development. However, the quality of titanium cast parts is not only determined by the interface reaction with the mould, but also by the surface quality and the reproduced shape details. The mould production by dip-coating is state-of-the-art. In order to further improve the precision of cast parts, calcium zirconate ($CaZrO_3$) coatings were manufactured via the replica technique, enabling functional coatings for titanium casting moulds by spraying and centrifuging [1]. Moreover, casting trials investigated the corrosion resistance of $CaZrO_3$ moulds, which were compared to a commercially available system containing silica. $CaZrO_3$ showed a very weak reaction, indicated by small oxygen contents and thereby low surface hardness of the titanium cast parts [2].

1 Introduction

As a near net shaping technology, investment casting enables the production of complex titanium cast parts, e.g. turbine blades, hip joints and jewellery. Titanium alloys are important for advanced applications in many industries, since they are lightweight, biocompatible and resistant to creep [3]. Titanium alloys are, however, extremely reducing and have a very high melting point. The corrosion reaction forms an oxygen-enriched surface called alpha case on the surface, which is hard and brittle [3–6]. Recently the high corrosion resistance of calcium zirconate ($CaZrO_3$) for titanium melting and casting was demonstrated [2, 7–8]. Containing a silica-free binder system, novel $CaZrO_3$ casting moulds were successfully developed according the lost-wax process [8].

The lost-wax process is state of the art for manufacturing investment casting moulds and comprises repeated dip-coating and stuccoing, drying, dewaxing and sintering. Afterwards, the metal melt is cast into the mould [3]. Especially the first coating layer of the ceramic mould determines the surface quality, since it is in direct contact with the melt during casting. However, dip-coating is limited regarding increasing demands on precision and complexity of shapes.

In order to reproduce intricate shapes with undercuts, different approaches should be favoured. The replica technique by Schwartzwalder characterises the manufacturing of macroporous ceramic foam filters [9], with the main application being metal melt filtration [10]. After coating of the polymeric foam, drying, burn-out of the foam and sintering take place. Various coating technologies such as centrifuging and

Lisa Freitag, Christos G. Aneziris
Institute of Ceramic, Glass and Construction Materials, TU Bergakademie Freiberg
09596 Freiberg
Germany

Florian Bulling, Ulrich E. Klotz
fem Research Institute for Precious Metals and Metals Chemistry
73535 Schwäbisch Gmünd
Germany

Stefan Schafföner
Department of Materials Science and Engineering
97 North Eagleville Road, Storrs
CT 06269, USA

Corresponding author: *L. Freitag*
E-mail: lisa.freitag@ikgb.tu-freiberg.de

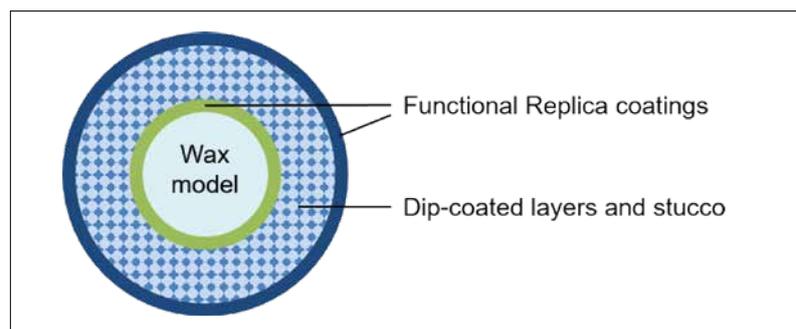Keywords: precision casting, titanium, coating

Fig. 1 Model of coating composition of investment casting moulds using functional layers

Tab. 1 Composition of the coating slips

Product Name	Imerys fused −45 μm	Stoichiometric, synthesized	Axilat RH 50 MD	Water	BYK LP-C 22134	BYK LP-C 22787	BYK LP-C 22893	BYK LP-C 22346
Raw Material	$CaZrO_3$	$CaZrO_3$	Xanthan gum	H_2O	Dispersing additive	Defoamer	Polymer binder	Polymer binder
Relative to solids:								
A [mass-%]	70	30	0,05	14	2	0,05	4	0
B [mass-%]	70	30	0,1	15	2	0,05	4	0
C [mass-%]	70	30	0,1	15	2	0,05	0	4

spraying can be used [10]. Both spraying and centrifuging produce thinner coating layers than dip-coating, whereas a sprayed coating can also be applied selectively. With these coating techniques, functional thin coatings could be used to improve the mould quality. A model of a graded composition with functional coatings is shown in Fig. 1.

In the present study, fine-grained $CaZrO_3$ coating slips for spraying and centrifuging were developed and evaluated regarding the rheology and coating properties with the aim of obtaining thin functional coatings.

Furthermore, the corrosion resistance against Ti–6Al–4V of the $CaZrO_3$-based shell material, produced by dip-coating, was compared to a conventional silica-based shell system, commercially available from the company Ransom & Randolph (R&R), Dentsply/US.

2 Materials and methods

2.1 Slip production

Tab. 2 provides the slip compositions. The used raw materials were fused $CaZrO_3$ (Imerys Fused Minerals Murg GmbH/DE) and stoichiometric $CaZrO_3$ by solid state synthesis as described in a previous study [8]. Xanthan gum (Axilat RH 50 MD, C.H. Erbslöh GmbH & Co. KG/DE) was used in order to modify the viscosity of the slurries. Hence, it was dissolved in water with a subsequent resting time of 2 h. Later on, the xanthan gum solution was mixed with a deflocculant (BYK LP-C 22134, BYK-Chemie GmbH, Germany) and a defoamer (BYK LP-C 22787, BYK-Chemie GmbH/DE) and subsequently added to the solids. After mixing the liquids for 5 min at a shear rate of 900 min⁻¹ using a high shearing laboratory mixer (RZR 2102 control, Heidolph Instruments GmbH & Co. KG/DE), an aqueous

polymer dispersion binder, i.e. BYK LP-C 22893, BYK-Chemie GmbH/DE for slips A and B or BYK LP-C 22346, BYK-Chemie GmbH/DE for slip C, was added, followed by mixing for 5 min at 900 min⁻¹. The slip was then mixed in a ball mill for at least 12 h and finally stirred again by the high shearing laboratory mixer for 5 min [1].

2.2 Coating production

Wax models are usually used for the production of investment casting moulds [3]. Regarding the coating experiments, wax models of Aqua Green Flake Wax (Freeman Manufacturing & Supply Company/US) with cylindrical or complex shapes were used. The coatings were applied on the wax models by different technologies. Dip-coating represented the reference coating technology. Therefore, the wax model was dipped into the ceramic slurry for an exact coating time of 10 s for complete wetting of all parts of the model with subsequent careful withdrawing and draining of the excess slip for 30 s. For centrifuging, dip-coating was also conducted, but the drain time was reduced to only 10 s. The excess slurry was then removed by an additional centrifuging step. Placing the coated model on a rotating disk fixed to a high shearing mixer, a rotational speed of 500 min⁻¹ was applied for a centrifuging time of 10 s. Regarding spraying, a spray gun (FB 150, Elektra Beckum/DE) having a nozzle diameter of 1,5 mm was used. In all cases, the spraying pressure was 3 bar and the spraying distance was about 20 cm, because these parameters ensured the ideal atomization of the slurry in preliminary experiments [1].

2.3 Coating investigations

Rheological investigations were conducted with the rotary rheometer HAAKE MARS 60 (Thermo Fisher Scientific Inc./US) and a profiled rotor (ZI 38 Ti) and pro-

filed beaker (ZI 43). The viscosity and shear stress values as a function of shear rate were measured at a constant temperature of 20 °C by applying an increasing shear rate of 0,1–100 s⁻¹ with 20 logarithmically distributed steps and a dwell time of 10 s for each step. Then, a dwell time of 60 s at 100 s⁻¹ was applied and afterwards the shear rate was decreased identically to the increase [1].

After the coating experiments, a minimum of five dried green samples of each composition were characterised. The applied mass was obtained by subtraction of the masses of the uncoated and coated models. Moreover, the coating thickness was determined by a digital Vernier caliper, measuring the diameters of the uncoated and coated models, respectively, and halving the subtracted values. Essentially the same part of each sample was measured. Furthermore, the coating quality, i.e. the adhesion, the cohesion and the homogeneity of the coatings, was evaluated subjectively after coating and drying. Selected coating surfaces were examined via Scanning Electron Microscopy (SEM) (XL30FEG, FEI Company/NL) for a better understanding of the microstructural differences of the coatings [1].

2.4 Casting trials

The shell mould system of $CaZrO_3$ was produced by dip-coating with two different grain sizes of the slurry: a fine-grained slurry with a maximum particle size of 0,5 mm and a coarse-grained slurry with a maximum particle size of 1 mm. The mould production was described in detail in another study [8].

The commercial silica-based shell system consisted of an yttria front coating and a stucco of alumina with a maximum particle size of 0,125 mm. Three layers were applied by dip-coating and sanded with kaolin stucco. After drying and dewaxing, the
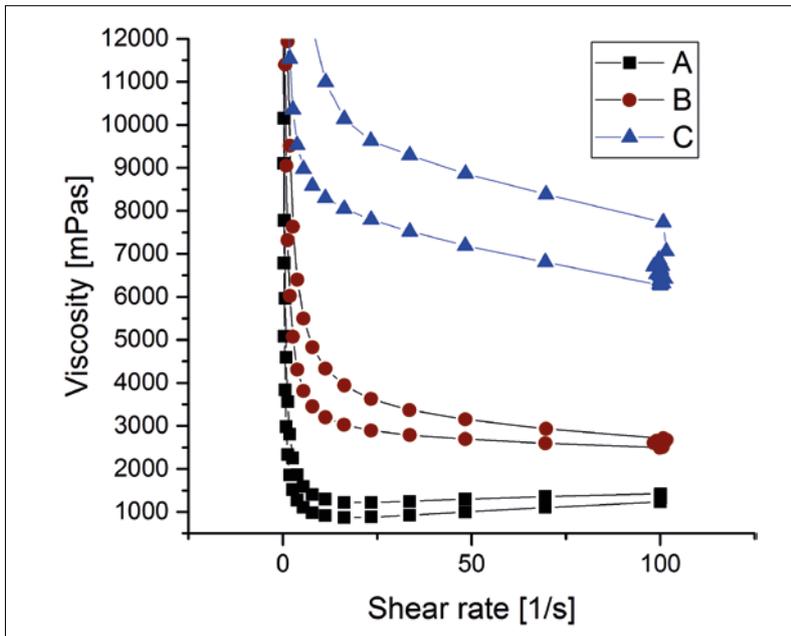
Fig. 2 Viscosity curves of the coating slips

moulds were sintered at a temperature of 930 °C [2].

Regarding the investment casting experiments, an electric arc furnace (LK6, ALD Vacuum Technologies GmbH/DE) was used for melting Ti–6Al–4V in in a cooled copper crucible. After melting, the titanium alloy was then tilt cast into the $CaZrO_3$ or commercial silica investment casting mould, respectively.

Reactions during melting were completely avoided due to the water-cooled crucible, an evacuation to $<5 \cdot 10^{-3}$ mbar and back-filling with argon to 400 mbar. All reactions of the metal were thus caused by the shell mould materials. In order to analyse the corrosion reaction at the interface, Vickers microhardness profiles were measured according to DIN EN ISO 6507-1 [2].

3 Results and discussions

3.1 Rheological investigations

Fig. 2 displays the viscosity curves of the different coating slips. There are clear differences between the coating slips, probably due to the influences of different compositions regarding the solids content, xanthan gum content and type of binder. The hysteresis loop of the viscosity curve, which is to some extent present for all coating slips, characterises the thixotropy. A certain thixotropy might improve the coating behaviour [1, 11].

Slip A, which had the highest solids content but a lower xanthan gum content, presented a slightly dilatant behaviour, as observed by the slight increase of the viscosity curve at shear rates higher than 25 s^{-1} (Fig. 2). This

changing behaviour from shear-thinning at low shear rates to Newtonian or dilatant at medium and higher shear rates is often reported for ceramic slips with a high solids content. By shearing the resting slurry, the particles are oriented into shear direction, but at higher shear rates the increased interaction of the particles contributed to a thickening effect in the slurry [1, 13].

Adding more water in order to adjust the rheology caused a shear-thinning behaviour, but not the required coating quality. Consequently, a higher amount of xanthan gum might be needed. In slip B, the combination of a higher xanthan gum content and a slightly higher water content seemed to improve the shear-thinning behaviour and also the sedimentation stability as well as the coating behaviour. Xanthan gum served both as a thickening agent and as a shear-thinning additive. These effects might have contributed to an improved coating behaviour [1, 12].

Furthermore, the effects of different binders on the viscosity were investigated. For the slips A and B, an aqueous urethane-acrylate dispersion binder was used, while slip C contained a solution of an acrylate co-polymer. The pure acrylate binder increased both the viscosity and also the thixotropy of slip C.

The high viscosity at low shear rates might have impaired the pumpability from a state of rest [13]. Hence, a lower concentration of this type of binder or a different binder should be preferred [1].

3.2 Coating properties

Tab. 2 presents the results of the coating experiments using different coating slips and coating technologies, whereas Fig. 3 shows centrifuged and sprayed coatings applied on a complex wax pattern using slip B.

Coating thickness and applied coating mass are important properties, which are linked if inhomogeneities or pores can be neglected [11]. However, the different slips and coating technologies have to be considered. Both novel coating technologies, i.e. spraying and centrifuging, always resulted in a lower applied coating mass and thinner coatings than dip-coating. Regarding the coating slurries, slip A yielded thicker coatings and a higher applied coating mass, probably due to the lack of the crucial shear-thinning behaviour [1].

Tab. 2 Properties of the green $CaZrO_3$ coatings

Coating Technology	Coating Slip	Applied Coating Mass [g]	Coating Thickness [mm]	Coating Quality
Dip-coating	A	4,5 ± 0,2	23,7 ± 0,4	−
Centrifuging	A	3,8 ± 0,2	25,8 ± 0,4	+
Spraying	A	2,9 ± 0,2	24,2 ± 2,6	−
Dip-coating	B	3,8 ± 0,2	29,7 ± 0,0	+
Centrifuging	B	7,2 ± 0,5	22,9 ± 0,5	++
Spraying	B	6,5 ± 0,2	23,7 ± 0,3	+
Dip-coating	C	5,6 ± 0,6	22,6 ± 0,2	+
Centrifuging	C	6,9 ± 0,4	27,1 ± 0,2	+
Spraying	C	10,4 ± 0,5	23,5 ± 1,3	−

The coating quality of different green $CaZrO_3$ coatings was macroscopically evaluated and by means of SEM with a focus on the coating adhesion, cohesion and homogeneity. First, the coating adhesion will be discussed. This property describes the adhesion of the coating layer on the wax pattern after coating, which is affected by the wetting behaviour and the external forces, such as the spraying pressure or the centripetal forces. The coating adhesion determines the inherent strength and is thus important to achieve homogeneity and mechanical strength [12]. Slip B applied by centrifuging yielded the best adhesion of all considered combinations. The high xanthan gum content of slip B contributed to a better adhesion, especially when external forces were applied. Moreover, the hydrophobic components of the associative binder in slip B might explain the better coating adhesion on the hydrophobic wax surface compared to slip C.

In all cases, centrifuging produced denser coatings compared to spraying. A reason might be the densification due to the centripetal forced and the accelerated drying of the thin coating. Spraying, by contrast, produced small slurry droplets by atomization. Hence, the coating consists of many droplets which have to coalesce after spraying [11]. Even if the wetting behaviour was suitable, which was the case for slip B, the bonding on the surface was rather weak and the droplets could be easily removed by abrasion.

The coating cohesion was similarly affected by the coating slip and the coating technology. It is defined as the internal bonding of
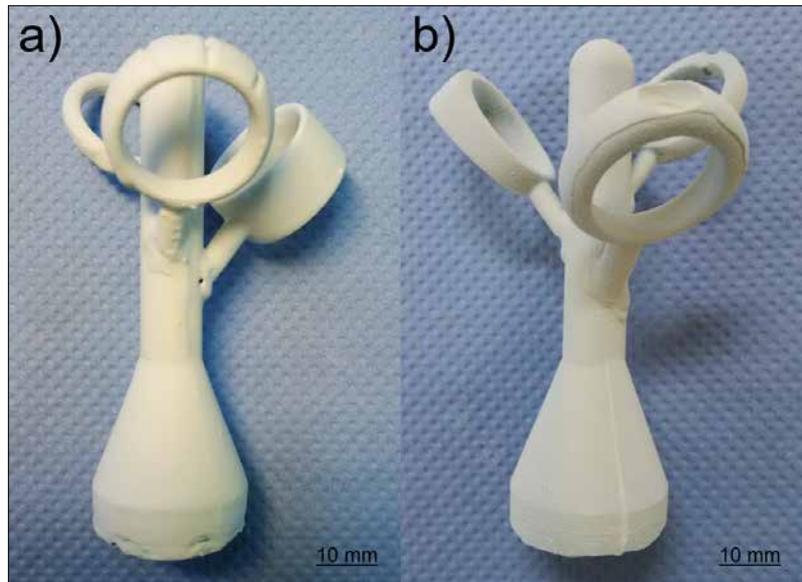

Fig. 3 Wax models used for jewellery casting coated with slip B:
a) coated by centrifuging, b) coated by spraying

the coating which was also improved by centrifuging with a suitable coating slurry. Furthermore, the homogeneity of the coatings was analysed. Slip A led to inhomogeneous coatings by sagging and slumping after dip-coating due to the less than ideal rheological behaviour. Slip B resulted in more homogeneous coatings. The homogeneity of spraying depended greatly on the slurry composition. This can be understood in view of the slurry rheology. Slip A was not shear-thinning at higher shear rates and slip C had a very high viscosity at the state of rest [1].

The microstructure of selected green samples is shown in Figs. 4–5. Fig. 4 presents a centrifuged coating of slip B. The surface

appears dense and smooth with some coarser grains and a fine-grained network of well-bonded particles. In comparison, the sprayed coating using slip B (Fig. 5) seems to have a rougher and rather loose microstructure. The sprayed droplets resulted in agglomerates of fine particles and some coarse particles without a distinct bonding [1].

Comparing the novel coating technologies, spraying should be preferred for very complex shapes and for selective application and centrifuging is more suitable for cohesive, dense and stable coatings with limited complexity. Both technologies are promising for the modification of investment casting moulds [1].
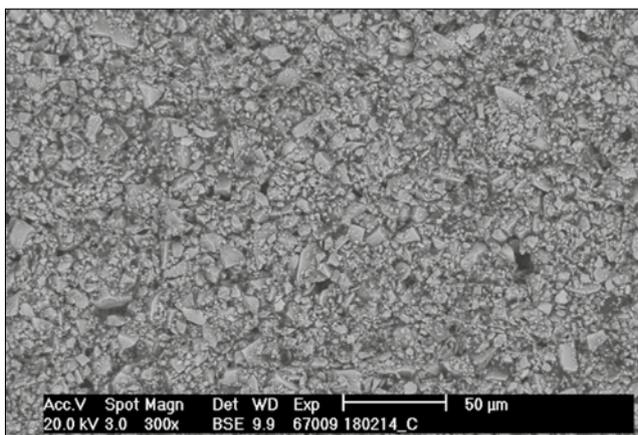

Fig. 4 SEM image of a functional green $CaZrO_3$, coating applied by centrifuging
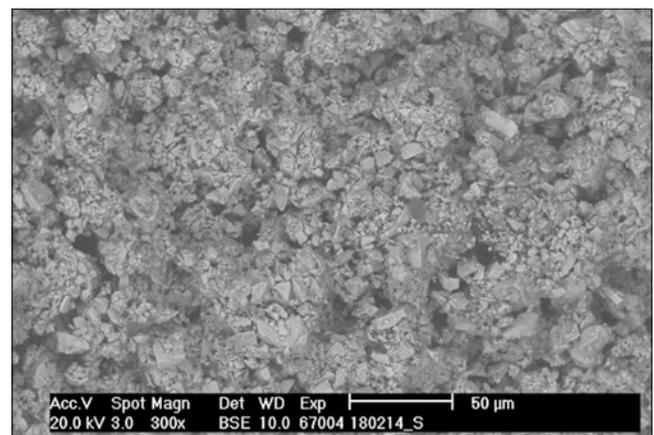

Fig. 5 SEM image of a functional green $CaZrO_3$, coating applied by spraying

3.3 Casting trials

Different shell mould materials were compared in order to understand the corrosion behaviour. The cast parts differed significantly regarding the reaction with the casting moulds. The silica-based shells had a strong adhesion of the shell material to the surface of the cast parts. In contrast, less adhesion was observed for the $CaZrO_3$ shells. Hardness profiles were measured in the reaction zone. The silica-based commercial mould caused a great hardness increase due to the diffusion of oxygen and aluminium from the surface to the core [2]. On the other hand, there was no significant effect on hardness by diffused zirconium or oxygen into the metal at cast parts using $CaZrO_3$-shells. The hardness in the core as well as on the surface was nearly the same, thus the formation of an α-case was successfully avoided by a $CaZrO_3$ shell material [2].

4 Conclusions

The study investigated novel coating technologies according the replica technique as potential coatings for $CaZrO_3$ based investment casting moulds. Furthermore, the corrosion resistance of the $CaZrO_3$ material war evaluated in comparison to a commercial mould material. It was shown that both the coating slurry and the coating technology greatly affect the coating quality. Using a suitable shear-thinning coating slip, spraying and centrifuging were successfully conducted. The coating thickness was significantly reduced compared to conventional dip-coating. Centrifuged coatings were denser with a better mechanical stability. Sprayed coatings had a weaker bonding, but they might be more promising for complex shapes [1].

Regarding the casting experiments, typical dip-coated shell moulds were used. The different compositions of the commercial silica-based mould and the newly developed $CaZrO_3$ shell mould resulted in different reactions with the titanium alloy TTi–6Al–4V. The typical α-case formation of titanium in
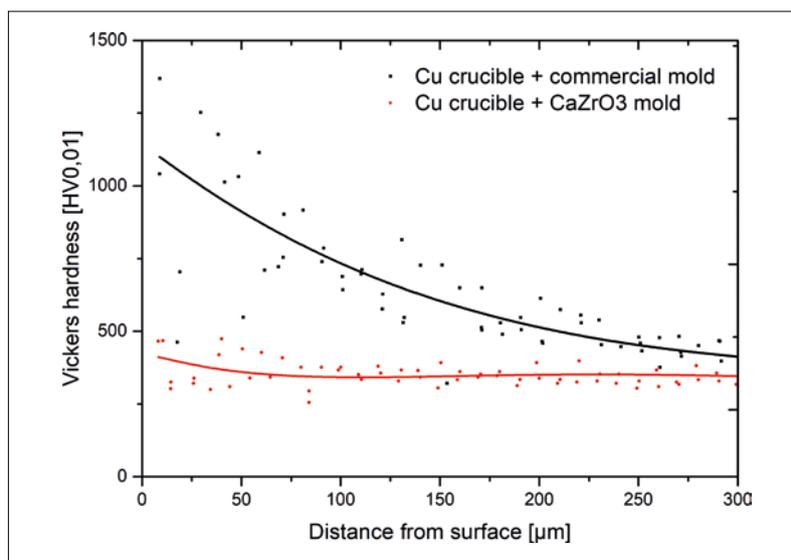

Fig. 6 Vickers microhardness profile of Ti–6Al–4V cast parts produced by melting in a cooled copper crucible and investment casting into a $CaZrO_3$ mould or commercial mould, respectively

contact with commercial investment material was avoided by using a $CaZrO_3$ shell system.

References

[1] Freitag, L.; et al: Functional coatings for titanium casting molds using the replica technique. J. Europ. Ceram. Soc. **38** (2018) 4560–4567

[2] Bulling, F.; et al.: Investment casting of titanium alloys with calcium zirconate moulds and crucibles. 61st Int. Coll. on Refractories 2018, Aachen, 27.–26.09.2018

[3] Beeley, P.R.; Smart, R.F. (eds.): Investment casting. The Institute of Materials, London 1995

[4] Frueh, C.; et al.: Attempts to develop a ceramic mould for titanium casting – a review. Int. J. Cast Met. Res. **9** (1996) 233–239

[5] Kim, S.K.; et al.: Investment casting of titanium alloys with CaO crucible and $CaZrO_3$ mold. Hoboken, NJ, 2001, 251–260, http://dx.doi.org/10.1002/9781118787922.ch23

[6] Klotz, U.E.; Heiss, T.: Evaluation of crucible and investment materials for lost wax investment casting of Ti and NiTi alloys. Int. J. Cast Met. Res. **27** (2014) 341–348

[7] Schafföner, S.; et al.: Investigating the corrosion resistance of calcium zirconate in contact with titanium alloy melts. J. Europ. Ceram. Soc. **35** (2015) 259–266

[8] Freitag, L.; et al.: Silica-free investment casting molds based on calcium zirconate. Ceram. Int. **43** (2017) 6807–6814

[9] Schwartzwalder, K.; Somers, H.; Somers, A.V.: Method of making porous ceramic articles, Patent US 3 090 094, 1963

[10] Voigt, C.; et al.: Investigations of reticulated porous alumina foam ceramics based on different coating techniques with the aid of μCT and statistical characteristics. Ceram. Int. **39** (2013) 2415–2422

[11] Reed, J.S.: Principles of ceramic processing, 2nd ed., New York, NY, 1995

[12] Tracton, A.A. (ed.): Coatings technology handbook. 3rd ed., Taylor & Francis Group, 2006

[13] Mezger, T.: The rheology handbook. 3rd ed., Hannover 2011

Developing the Powder Metallurgy Future

european powder
metallurgy association

30 YEARS
CELEBRATING
EPMA
european powder metallurgy association

International Congress & Exhibition

13 – 16 October 2019

Maastricht Exhibition & Congress Centre (MECC),
Maastricht, The Netherlands

**EURO
PM2019**
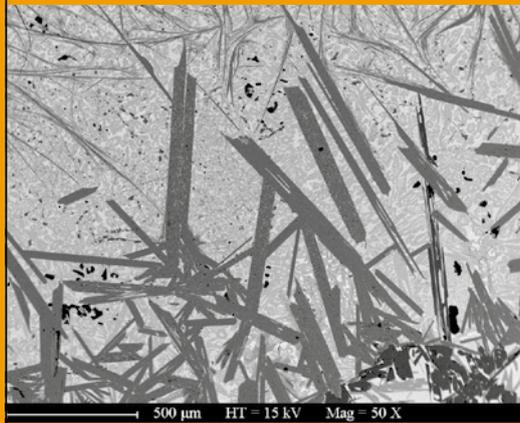CONGRESS & EXHIBITION

EURO
PM2019
CONGRESS & EXHIBITION

www.europm2019.com